Advances in Concrete Construction, *Vol. 2, No. 3 (2014) 177-192*
DOI: http://dx.doi.org/10.12989/acc.2014.2.3.177

Experimental investigation of the stress-strain behavior of FRP confined concrete prisms

F. Hosseinpour[*1] and R. Abbasnia[2a]

[1]*Herff College of Engineering, University of Memphis, Memphis, TN 38152, USA*
[2]*Department of Civil Engineering, Iran University of Science and Technology, Tehran 16844, Iran*

(Received February 21, 2013, Revised July 27, 2014, Accepted August 1, 2014)

Abstract. One of the main applications of FRP composites is confining concrete columns. Hence identifying the cyclic and monotonic stress-strain behavior of confined concrete columns and the parameters influencing this behavior is inevitable. Two significant parameters affecting the stress-strain behavior are aspect ratio and corner radius. The present study aims to scrutinize the effects of corner radius and aspect ratio on different aspects of stress-strain behavior of FRP confined concrete specimens (rectangular, square and circular). Hence 44 FRP confined concrete specimens were tested and the results of the tests were investigated. The findings indicated that for specimens with different aspect ratios, the relationship between the ultimate stress and the corner radius is linear and the variations of the ultimate stress versus the corner radius decreases as a result of an increase in aspect ratio. It was also observed that increase of the corner radius results in increase of the compressive strength and ultimate axial strain and increase of the aspect ratio causes an increase of the ultimate axial strain but a decrease of the compressive strength. Investigation of the ultimate condition showed that the FRP hoop rupture strain is smaller in comparison with the one obtained from the tensile coupon test and also the ultimate axial strain and confined concrete strength are smaller when a prism is under monotonic loading. Other important results of this study were, an increase in the axial strain during the early stage of unloading paths and increase of the confining effect of FRP jacket with the increase and decrease of the corner radius and aspect ratio respectively, a decrease in the slope of reloading branches with cycle repetitions and the independence of this trend from the variations of the aspect ratio and corner radius and also quadric relationship between the number of each cycle and the plastic strain of the same cycle as well as the independence of this relationship from the aspect ratio and corner radius.

Keywords: FRP confined concrete; corner radius; aspect ratio; cyclic and monotonic loadings; stress-strain behavior

1. Introduction

Retrofitting of concrete columns is a subject that has long been of special interest. So far several methods have been utilized to retrofit of the concrete columns. One of the most efficient strategies for enhancing both ultimate strength and ductility of the concrete columns, being used since the 1990s, is FRP confining. Some researchers investigated the stress-strain behavior of FRP

*Corresponding author, PhD Student, E-mail: Fhssnpur@memphis.edu
[a]Associate Professor

http://www.techno-press.org/?journal=acc&subpage=7 ISSN:2287-5301(Print)2287-531X(Online)

confined concrete specimens under the action of cyclic and monotonic loadings. Although a lot of studies have been dedicated to the investigation of the monotonic stress-strain behavior of FRP confined concrete specimens, the cyclic stress-strain behavior FRP confined concrete specimens, except in few cases, is less considered. It can be concluded from the research that there are several parameters which affect the stress-strain behavior of FRP confined concrete specimens. Two important parameters affecting the stress-strain behavior are aspect ratio and corner radius. Hence the present study has shed some light on the effects of the aspect ratio and corner radius on the different aspects of monotonic and cyclic stress-strain behavior of FRP confined concrete specimens.

2. Literature review

There are some studies investigating the effects of the corner radius on the monotonic and cyclic stress-strain behavior of FRP confined concrete specimens. Mirimiran *et al*. (1998) examined the effect of the corner radius on the effectiveness of square jacket under the action of monotonic loading and suggested that the increase of corner radius leads to the increase of the effectiveness of square jacket. Rochette and Labossie`re (2000) studied the effect of the corner radius on the monotonic stress-strain curve. They concluded that the variations of the corner radius have a direct effect on the stress-strain behavior and demonstrated that with the increase of corner radius, the stress-strain curve tends toward an ascending behavior (hardening behavior) and with the decrease of the corner radius, it tends toward a descending behavior (softening behavior). Wang and Wu (2008) investigated the monotonic stress-strain behavior of square prisms with different corner radii and concluded that the variations of the corner radius have a great impact on the strength and ductility of confined prisms. They demonstrated that the increase of corner radius leads to the increase of confined concrete strength. They also showed that the effect of corner radius on the strength of the jackets with sharp corners is trivial but it has a significant effect on their ductility. Al-Salloum (2007) also studied the monotonic stress-strain behavior of square prisms with different corner radii and presented a modified analytical model to predict the strength of the square prisms. He indicated that the corner radius has a direct impact on the efficiency of FRP confinement and increasing of the corner radius results in delaying the rupture of the FRP composite at the edges. Abbasnia *et al*. (2012) and studied previous monotonic researches and investigated the effect of the corner radius on some aspects of the cyclic loading and concluded that the variations of the corner radius do not affect the plastic strain, stress deterioration ratio and relationship between cyclic and monotonic stress-strain curves. They also argued that with increase of the corner radius, the failure area increases. There are also some studies investigating the effects of the aspect ratio on the monotonic and cyclic stress-strain behavior of FRP confined concrete specimens. Rochette and Pierre Labossie`re (2000) examined the stress-strain behavior of the rectangular columns confined with composites under the action of monotonic loading and found that the shape of the cross section directly influences the confinement effect. Lam and Teng (2003) studied the stress-strain behavior of FRP confined concrete rectangular prisms and presented a simple design-oriented stress-strain model. Based on their model, there is an inverse relationship between aspect ratio and the compressive strength but the increase in the aspect ratio increases the ultimate axial strain. Wu and Wei (2010) investigated the effect of the aspect ratio on the monotonic compressive strength of CFRP-confined rectangular concrete columns and indicated that the increase of the aspect ratio results in a decreased compressive strength. They also presented a strength model which was in a good agreement with performed experimental

studies. Abbasina *et al*. (2012) and also scrutinized the effect of the aspect ratio on different aspects of cyclic stress-strain behavior. They suggested that the plastic strain, stress deterioration ratio and the relationship between monotonic and cyclic stress strain curves are unaffected by the variations of the aspect ratio.

3. Experimental work

In this investigation 44 FRP confined concrete specimens with different corner radii and aspect ratios were tested. In the first step, the concrete molds made from medium density fiberboard (MDF) wood were prepared for casting. The edge sharpness of the cross section for each specimen was obtained by a polyvinyl chloride (PVC) pipe divided into four quadrants with desired corner radius and height. In the next step the concrete specimens were made for nominal 28-day design strength of 25 MPa. For each batch of concrete, three control cylindrical specimens were prepared. A summary of concrete mix design proportions is presented in Table 1. 24 hours after casting, the specimens were removed from the molds and put in water for 28 days to cure.

After 28 days the specimens were removed from the water and after their surface was smoothed and cleaned, they were left to dry. Afterward the specimens were prepared for FRP wrapping. Then each specimen was wrapped in two layers of CFRP (Carbon Fiber Reinforced Polymer) and a single lap of 150 mm long using wet lay-up process. Table 2 shows the mechanical properties of CFRP. The last step before testing the specimen was strain gauge installation. For each specimen, two strain gauges mounted at 180o apart were used to measure lateral strains. Fig. 1 illustrates installation steps of strain gauges. On the test day the specimens were placed in a frame similar to that designed by Wang and Wu (2008). Two linear variable displacement transducers (LVDTs) were also mounted at 180o apart on the frame to measure axial strains and also a load cell with a capacity of 200 ton was used to measure the axial load (see fig. 2). The data obtained from load cell, strain gauges and LVDTs were recorded by a data logger.

The patterns of loading are also showed in fig. 3. To obtain the compressive strength of the specimens on the day of testing, the control columns were tested at first and their compressive strength were 30 to 33 Mpa. Testing of the FRP confined concrete specimens revealed that the failure of the specimens was with a sudden and explosive sound and was mainly due to tensile lateral strains developed under compressive axial strains at the middle portion of the specimens. The results of the tests are presented below.

Table 1 Concrete mix design

Coarse aggregate (kg/m3)	Fine aggregate (kg/m3)	Cement (kg/m3)	Water (kg/m3)	Water to Cement ratio	28-day strength of concrete (Mpa)
1038	808.5	330	198.4	0.61	25

Table 2 Mechanical properties of CFRP

Specimen type	Primary fiber direction	Nominal thickness (mm)	Elastic modulus (Gpa)	Tensile strength (MPa)	Ultimate tensile strain (%)
CFRP laminate			241	3943.5	1.63

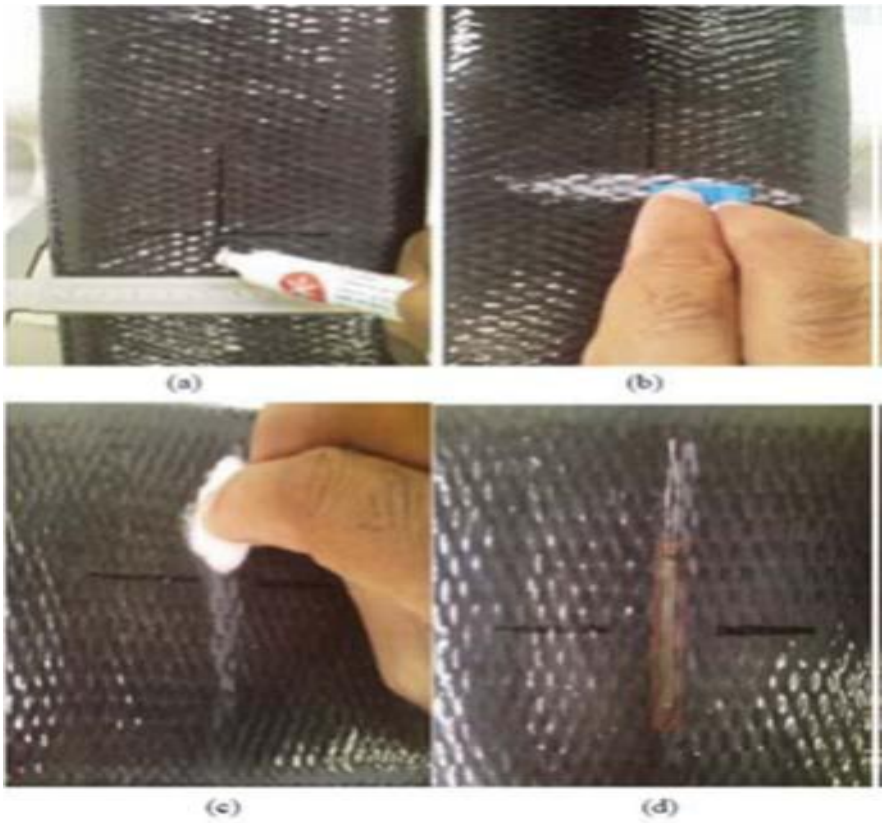

Fig. 1 Installation steps of strain gauges

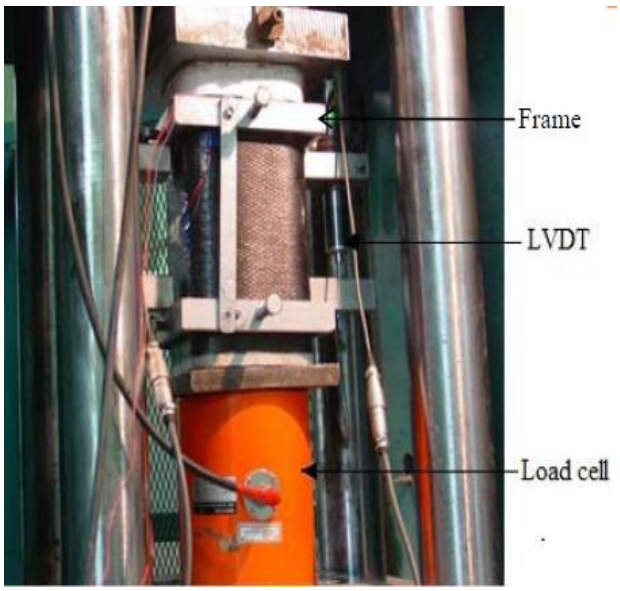

Fig. 2 Test setup and instrumentation

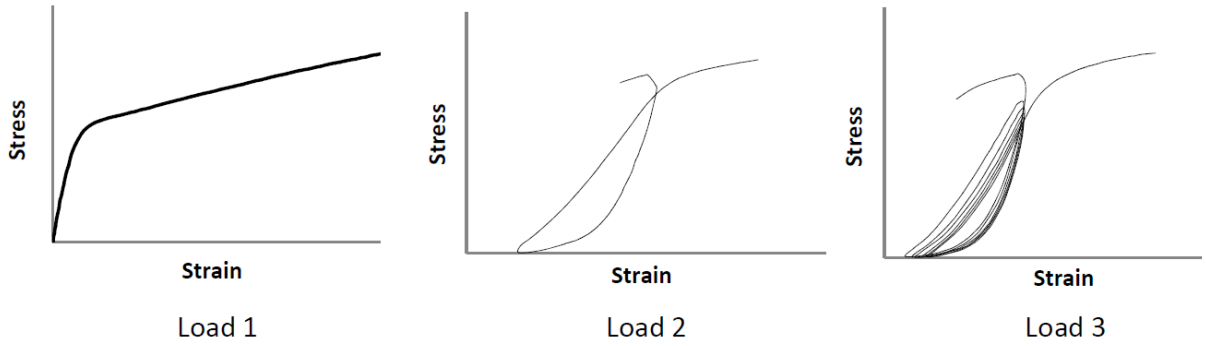

Fig. 3 Loading patterns

(Load 1) Monotonic loading (Load 2) Cyclic loading involving a single complete unloading/reloading cycle at each prescribed displacement level (Load 3) Cyclic loading involving several complete unloading/reloading cycles at each prescribed displacement level

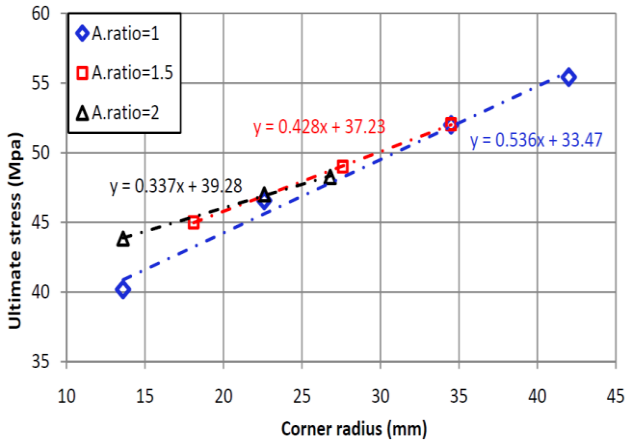

(a) Load 1

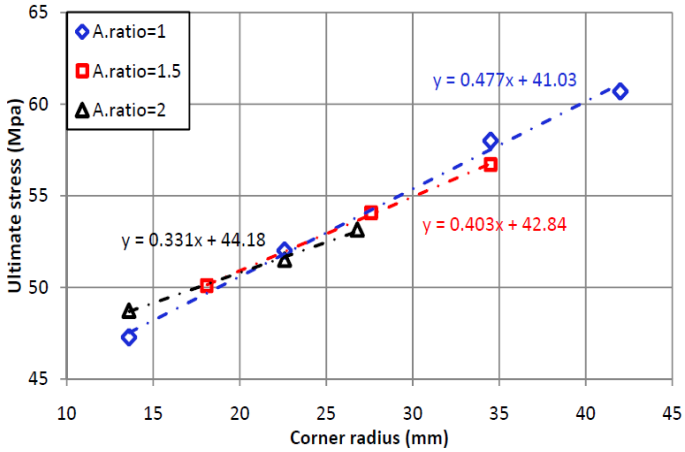

(b) Load 2

Fig. 4 Simultaneous effect of corner radius and aspect ratio on the ultimate stress

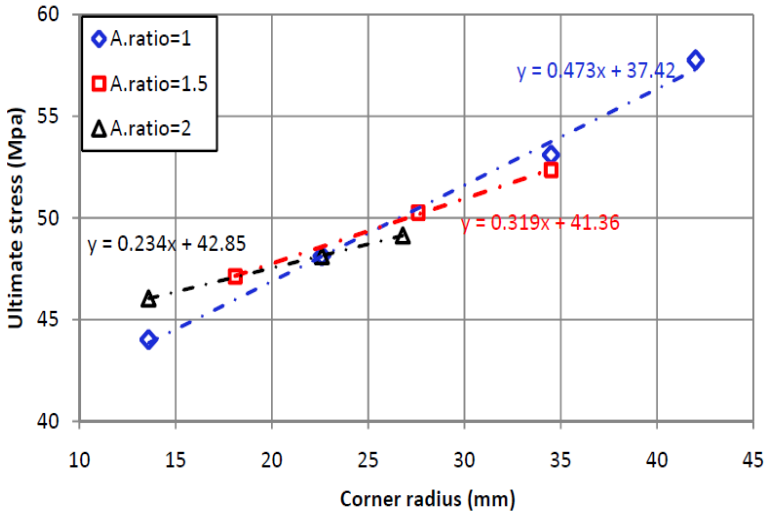

(c) Load 3

Fig. 4 Continued

Table 3 Details of FRP-confined specimens and key test results

Prism	Dimension (mm)	Corner radius (mm)	Unconfined Concrete strength f'_{co} (Mpa)	Loading type	Confined concrete strength f'_{cc} (Mpa)	Ultimate axial strain ε_{cu}	FRP hoop rupture strain $\varepsilon_{h,rup}$
No-1	150×150×300	13.6	30	Load 1	40.19	0.0141	0.0106
No-2	150×150×300	22.6	30	Load 1	46.58	0.0125	0.0098
No-3	150×150×300	34.5	30	Load 1	52.01	0.0114	-[a]
No-4	150×150×300	42	30	Load 1	55.42	0.0107	0.0102
No-5	120×180×300	18.1	30	Load 1	45.01	0.0162	0.0119
No-6	120×180×300	27.6	30	Load 1	49	0.0143	-[a]
No-7	120×180×300	33.6	30	Load 1	52.04	0.0134	0.0109
No-8	90×180×300	13.6	30	Load 1	43.85	0.01776	0.0120
No-9	90×180×300	20.7	30	Load 1	47.02	0.01558	0.0108
No-10	90×180×300	25.2	30	Load 1	48.27	0.0139	-[a]
No-11	cylindrical	75	30	Load 1	73.77	0.0209	-[a]
No-12	150×150×300	13.6	33	Load 2	47.28	0.0165	0.0114
No-13	150×150×300	22.6	33	Load 2	52.01	0.0176	0.0123
No-14	150×150×300	34.5	33	Load 2	58	0.0151	-[a]
No-15	150×150×300	42	33	Load 2	60.69	0.0146	0.0111
No-16	120×180×300	18.1	33	Load 2	50.10	0.0185	0.0127
No-17	120×180×300	27.6	33	Load 2	54.07	0.0174	0.0119
No-18	120×180×300	33.6	33	Load 2	56.7	0.0166	-[a]
No-19	90×180×300	13.6	33	Load 2	48.73	0.0205	0.0131
No-20	90×180×300	20.7	33	Load 2	51.52	0.0193	0.0123
No-21	90×180×300	25.2	33	Load 2	53.16	0.0189	0.0117
No-22	cylindrical	75	33	Load 2	79.14	0.0227	0.0140
No-23	150×150×300	13.6	30	Load 2	43.76	0.016	-[a]

Table 3 Continued

Prism	Dimension (mm)	Corner radius (mm)	Unconfined Concrete strength f'_{co} (Mpa)	Loading type	Confined concrete strength f'_{cc} (Mpa)	Ultimate axial strain ε_{cu}	FRP hoop rupture strain $\varepsilon_{h,rup}$
No-24	150×150×300	22.6	30	Load 2	50.16	0.0153	0.0124
No-25	150×150×300	34.5	30	Load 2	55.61	0.0142	0.0113
No-26	150×150×300	42	30	Load 2	58.92	0.0138	-a
No-27	120×180×300	18.1	30	Load 2	48.14	0.0184	0.0128
No-28	120×180×300	27.6	30	Load 2	51.25	0.0148	0.0117
No-29	120×180×300	33.6	30	Load 2	54.04	0.0152	0.0110
No-30	90×180×300	13.6	30	Load 2	47.17	0.0181	-a
No-31	90×180×300	20.7	30	Load 2	48.89	0.0179	0.0123
No-32	90×180×300	25.2	30	Load 2	49.91	0.0172	0.0128
No-33	cylindrical	75	30	Load 2	75.02	0.0191	0.0133
No-34	150×150×300	13.6	30	Load 3	44.01	0.0171	0.0124
No-35	150×150×300	22.6	30	Load 3	48.13	0.0141	-a
No-36	150×150×300	34.5	30	Load 3	53.09	0.0156	0.0116
No-37	150×150×300	42	30	Load 3	57.76	0.0140	0.0113
No-38	120×180×300	18.1	30	Load 3	47.12	0.0177	0.0126
No-39	120×180×300	27.6	30	Load 3	50.25	0.171	0.0117
No-40	120×180×300	33.6	30	Load 3	52.35	0.0151	-a
No-41	90×180×300	13.6	30	Load 3	46.04	.0191	0.0127
No-42	90×180×300	20.7	30	Load 3	48.13	0.0182	0.0124
No-43	90×180×300	25.2	30	Load 3	49.13	0.0167	-a
No-44	cylindrical	75	30	Load 3	75.91	0.0214	0.0136

[a] No strain gauges were bonded

4. Test results

4.1 Simultaneous effect of aspect ratio and corner radius on ultimate stress

To have a proper design of FRP confined concrete specimens, it is necessary to know the stress-strain behavior of the specimens and also the impact of the effective parameters on this behavior. To have a better vision for designing FRP confined concrete, we need to know simultaneous influence of the effective parameters. The combined effect of corner radius and aspect ratio is an issue that does not seem to have properly been examined. Hence in this study the simultaneous effect of the aspect ratio and corner radius on the ultimate stress was investigated and the diagram of the ultimate stress versus corner radius for specimens with different aspect ratios was obtained (see fig. 4). As can be seen in fig. 4, the correlation between the ultimate stress and corner radius is linear for prisms with different aspect ratios. Fig. 4 also indicates that with the increase of the aspect ratio, the variations of the ultimate stress versus the corner radius decreases; that is, the effect of the corner radius on the increase of the ultimate stress has an inverse relationship with the aspect ratio. Having more reasonable results calls for more experimental investigations on the combined effect of these parameters.

4.2 Ultimate condition

As the eventual failure of FRP-confined concrete is due to the rupture of FRP jacket, the ultimate condition of the confined concrete, often characterized by its compressive strength and ultimate axial strain, is intimately related to the ultimate tensile strain or tensile strength of the confining FRP jacket in the hoop direction (Lam and Teng 2004). Many predicted models of ultimate condition seem to suffer from some deficiencies. In many of these models it is assumed that FRP rupture occurs as the FRP hoop stress reaches the tensile strength from coupon tensile test and in some other models the effect of jacket stiffness was not explicitly considered. On the other hand most of the predicted models of ultimate strain and compressive strength are related to monotonic loading and fewer studies have been conducted on cyclic loading. Hence a large test database is required to predict the monotonic and cyclic ultimate strain and compressive strength truly. To investigate the cyclic and monotonic ultimate condition of FRP confined concrete specimens with different corner radii and aspect ratios, the compressive strength and ultimate axial strain of the specimens were obtained and compared with each other. Table 3 shows details of FRP-confined specimens and key test results. As it can be seen in Table 3, with increase of the corner radius, the compressive strength and ultimate axial strain increases and with increases of aspect ratio, the compressive strength decreases but ultimate axial strain increases. It can also be concluded that the FRP hoop strain at rupture is typically lower than the ultimate tensile strain in the coupon tensile test. Comparing the monotonic and cyclic test results, it can be observed that the axial strain and compressive strength related to monotonic loading are lower than those of cyclic loading. More examination of the ultimate condition and providing a reliable model require more experimental studies.

4.3 Increase of axial strain in the envelope unloading path

Examination of cyclic stress-strain curve of FRP confined concrete prisms showed a rise in the unloading strain in the early stage of unloading path which can be due to inhibitory effect of FRP jacket against the dilation and lateral expansion of concrete core. Mirmiran and Shahawy (1997) examined this issue for circular specimens and defined the dilation rate as the tangent Poisson's ratio or the rate of change of lateral strains with respect to axial strains and used the Eq. (1) to calculate the experimental dilation rate:

$$\mu_{exp} = \frac{\Delta\varepsilon_r}{\Delta\varepsilon_c} \tag{1}$$

where $\Delta\varepsilon_r$ and $\Delta\varepsilon_c$ are two consecutive lateral and axial strains respectively. They also presented a typical plot of dilation rate versus axial strain (see fig. 5) and divided the dilation curve into three regions. They showed that the first region is the same as plain concrete, because the lateral expansion of the core is negligible. The second region is transition zone and is due to development of micro cracks in the concrete core which causes an increase of lateral expansion to a peak value of μ_{max}. Finally, the third recognized region in which the jacket assumes full control of lateral expansion and dilation rate becomes stable to an asymptotic value of μ_u (Mirmiran and Shahawy 1997). To investigate this issue for rectangular and square specimens and examine the effect of the corner radius and aspect ratio on this behavior, the unloading and maximum

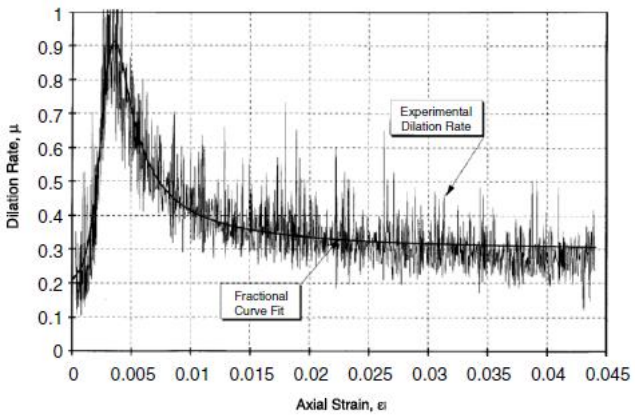

Fig. 5 Typical dilation rate for FRP-encased concrete (Mirmiran and Shahawy 1997)

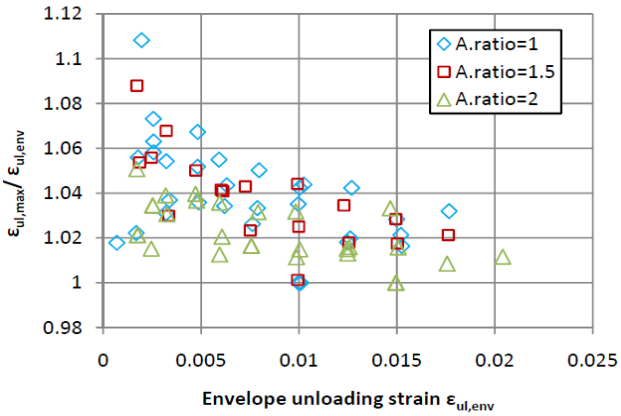

(a) Different aspect ratios

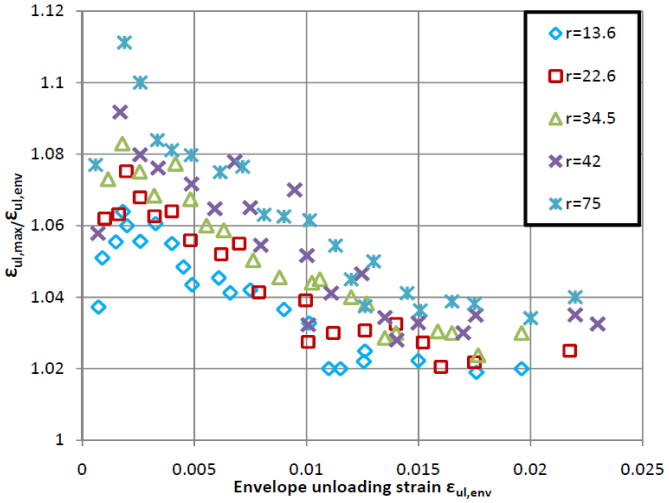

(b) Different corner radii

Fig. 6 Correlation between εul,max/εul,env and εul,env for specimens with

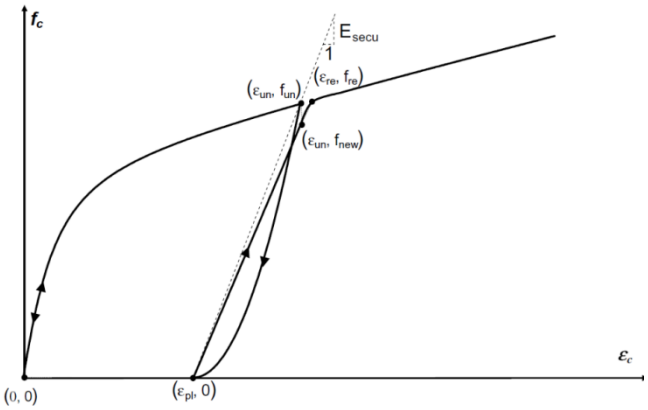

Fig. 7 unloading and reloading between envelope curve and zero stress (Shao *et al*. 2006)

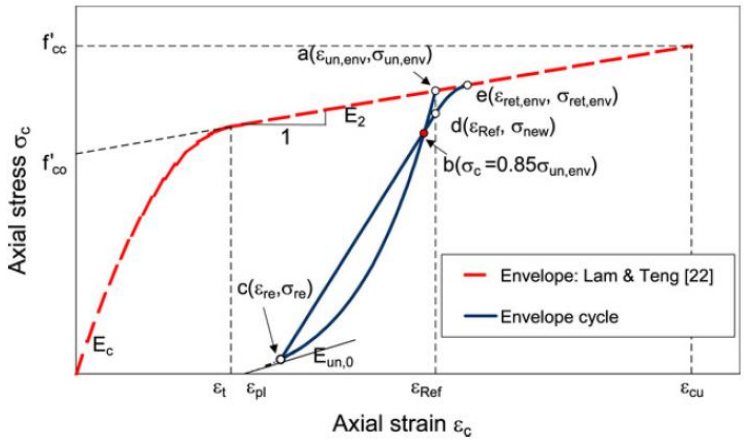

Fig. 8 Key parameters of cyclic stress–strain curves of FRP-confined concrete (Lam and Teng 2009)

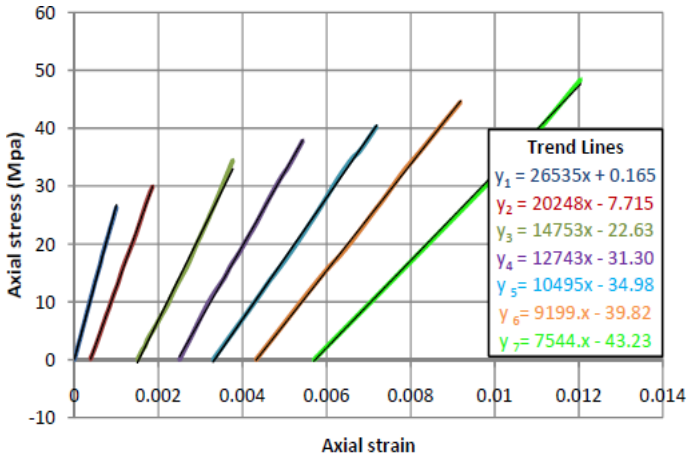

(a) Specimen No-25

Fig. 9 Reloading branches

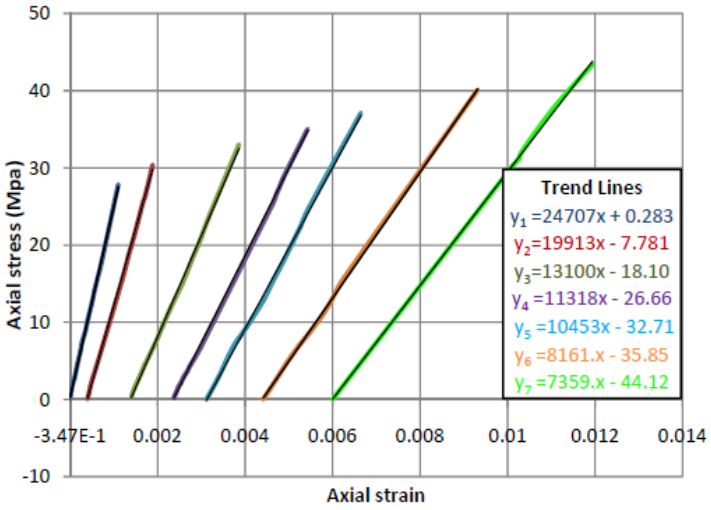

(b) Specimen No-28

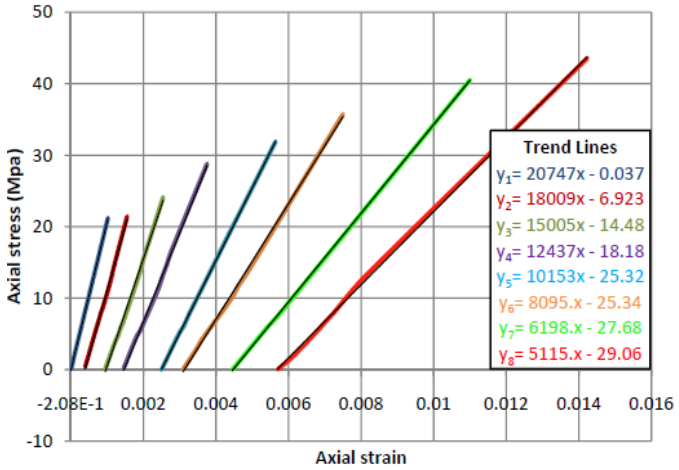

(c) Specimen No-32

Fig. 9 Continued

unloading strains of loading-unloading cycles were obtained and the diagram of $\frac{\varepsilon_{ul,max}}{\varepsilon_{ul,env}}$ versus $\varepsilon_{ul,env}$ was depicted (see fig. 6). As it can be seen in fig. 6 the maximum strain and unloading strain are almost the same at first but then the ratio of maximum strain to unloading strain increases gradually (due to increases of the reaction of jacket to lateral expansion) until it reaches to a maximum value and after that follows a downward trend until it reaches to a constant value. Fig. 6 shows a similar trend for prisms with different corner radii and aspect ratios. It can also be inferred that the ratio of $\frac{\varepsilon_{ul,max}}{\varepsilon_{ul,env}}$ in a specific unloading strain increases with the increase and decrease of the corner radius and aspect ratio respectively. Hence it can be concluded that the variations of the corner radius and aspect ratio directly affect the confining effect of the FRP jacket.

4.4 Effect of cycle repetitions on the slope of the reloading path

Examination of the previous studies shows that reloading path is generally linear. Shao *et al* (2006) predicted the reloading paths linearly. To determine the reloading path in the Shoa *et al*'s model, one of the main parameters is the new stress at the envelope unloading strain (f_{new}), which is obtained from the Eq. (2)

$$f_{new} = 0.9 f_{un,env} \tag{2}$$

Shao suggested that the first portion of the reloading path is a path connecting the point of zero stress to the point of f_{new} (see fig. 7). For the second portion, they assumed that the reloading branch extends to the envelope curve (f_{re}, ε_{re}) with the same slope as the first portion. Lam and Teng (2009) also suggested that the reloading branch consists of a linear and a parabolic portion. They indicated that the first portion of the reloading branch is linear (point 'c' to point 'd' in fig. 8), as it was said in the shao *et al*. model (2006), and suggested the Eq. (3):

$$\sigma_c = \sigma_{re} + E_{re}(\varepsilon_c - \varepsilon_{re}) \quad (\varepsilon_{re} \le \varepsilon_c \le \varepsilon_{ref}) \tag{3}$$

where σ_{re} and ε_{re} are the stress and strain at the starting point of the reloading path respectively. If the σ_{re} is considered zero, in other words, the reloading path starts from the point of zero stress, then the Eq. (3) can be considered as follows (Eq. (4)):

$$\sigma_c = E_{re}(\varepsilon_c - \varepsilon_{re}) \tag{4}$$

where E_{re} is the slope of the linear portion and is found from Eq. (5):

$$E_{re} = \frac{(\sigma_{new} - \sigma_{re})}{(\varepsilon_{ref} - \varepsilon_{re})} \quad (\varepsilon_{re} \le \varepsilon_c \le \varepsilon_{ref}) \tag{5}$$

where σ_{new} and ε_{ref} are new stress at the envelope unloading strain and envelope unloading strain respectively.

They also showed that the assumption of the shoa *et al*'s model for the second portion is not valid anymore and suggested the Eq. (6) for the parabolic portion (point'd' to point 'e' in fig. 8):

$$\sigma_c = \mathrm{A}\varepsilon_c{}^2 + \mathrm{B}\varepsilon_c + C \quad (\varepsilon_{ref} \le \varepsilon_c \le \varepsilon_{ret,env}) \tag{6}$$

where A, B and C are constants to be determined and $\varepsilon_{ret,env}$ is envelope returning point. In the present study the slope of linear portion was investigated for specimens with different corner radii and aspect ratios and the effect of cycle repetitions on the slope of the linear portion of reloading branch was examined. For this purpose, the linear portion of reloading branches depicted separately for each specimen and the linear equation of each reloading path was obtained (see fig. 9). As can be seen in the fig. 9, the slope of the reloading branches decreases with the repetition of the cycles. This indicates that FRP confined concrete specimen shows resistance to longitudinal strains at first and with increase of cycle repetitions, longitudinal strains increases gradually until it ruptures. It can also be concluded that the variations of the corner radius and aspect ratio do not have any effect on this trend or in other words for specimens with different corner radii and aspect ratios, the slope of the reloading path decreases gradually with increase of cycle repetitions.

4.5 Effect of number of cycles on the plastic strain

One of the most significant parameters for modeling the cyclic stress-strain behavior of the FRP confined concrete specimens is the plastic strain. The relationship between plastic strain and envelope unloading strain and the effect of corner radius, aspect ratio and number of FRP layers on the plastic strain are the issues that have been considered more or less. Another aspect of cyclic loading including plastic strain investigated in the present study is the effect of the number of cycles on the plastic strain. To this purpose, for each cycle, the plastic strain was obtained. Fig. 10 illustrates the correlation between the number of cycles and the plastic strain of the same cycle. As it can been seen the relationship can be considered by a polynomial trend line of order two with relatively high accuracy. In order to obtain a reliable quadric equation indicating the relationship which considers all the parameters affecting the stress-strain behavior of FRP confined concrete correctly, more research needs to be done. To examine the effect of the corner radius and aspect ratio on the relationship between the number of cycles and the plastic strain, for each certain cycle, the plastic strain for specimens with different corner radii and aspect ratios was obtained and compared with each other (see fig. 11). As the fig. 11.a indicates, in a certain cycle, with negligible loss of accuracy, the plastic strain is the same for specimens with different corner radii. Fig. 11.b also shows similar results for prisms with different aspect ratios. Hence it can be concluded that the variations of the corner radius and aspect ratio do not have any significant effect on the correlation between the number of cycles and the plastic strains. Lack of information in this field calls for more prospective studies.

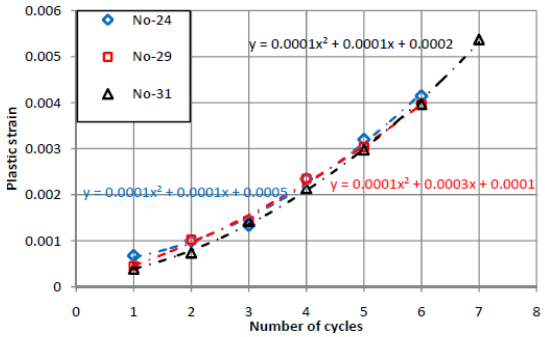

Fig. 10 Correlation between number of cycles and plastic strain

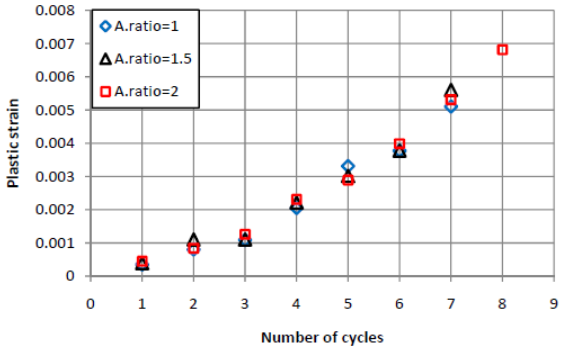

(a) Different aspect ratios

Fig. 11 Number of cycles versus plastic strain for specimens with:

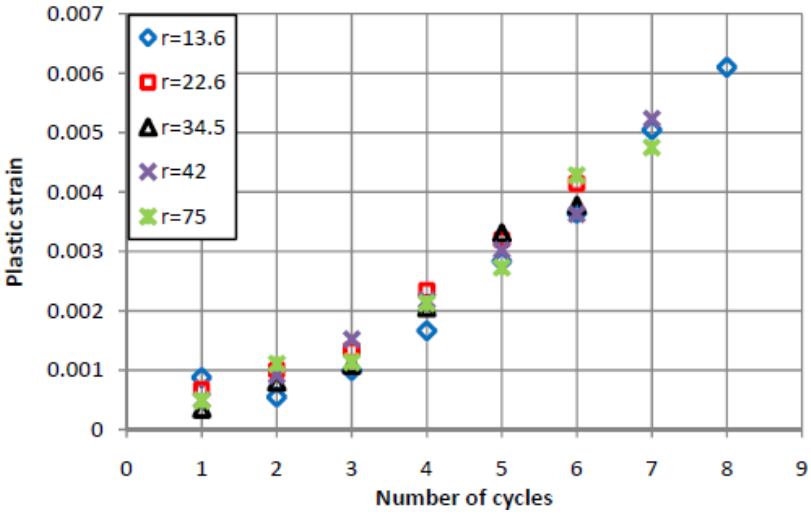

(b) Different corner radii

Fig. 11 Continued

5. Conclusions

The main concern of this paper has been the cyclic and monotonic stress-strain behavior of FRP confined concrete specimens (circular, square and rectangular specimens) and the effect of corner radius and aspect ratio on this behavior. The findings presented in this paper allow the following conclusions to be drawn:

(1) The ultimate stress and corner radius have a linear relationship for specimens with different aspect ratios and as the aspect ratio increases, the effect of corner radius on the ultimate stress decreases.

(2) The compressive strength and ultimate axial strain increase with increase of the corner radius, and with increases of the aspect ratio, the compressive strength decreases but ultimate axial strain increases.

(3) In specimens with different corner radii and aspect ratios, FRP hoop rupture strain is smaller than the one of tensile coupon test and for specimens under monotonic loading, ultimate axial strain and confined concrete strength is smaller as opposed to when they are under cyclic loading.

(4) There is an increase in unloading strain in the early stage of unloading branch in specimens with different corner radii and aspect ratios which can be as a result of inhibitory effect of FRP jacket against the dilation and lateral expansion of concrete core.

(5) The confining effect of the FRP jacket increases with the increase and decrease of the corner radius and aspect ratio respectively.

(6) Cycle repetitions result in decrease of the slope of reloading branches and this trend is similar for different corner radii and aspect ratios.

(7) The relationship between the number of cycles and the plastic strain of the same cycle is polynomial of order two and is independent from the corner radius and aspect ratio.

Acknowledgments

The authors are grateful for the financial support provided by Iran University of Science and Technology. Thanks are also extended to the technicians of the Structural Laboratory at the College of Civil Engineering, Iran University of Science and Technology for their invaluable contribution to the experimental work.

References

Mirmiran, A., Shahawy, M., Samaan, M. and El Echary, H. (1998), "Effect of column parameters on FRP-confined concrete", *J. Compos. Constr., ASCE*, **2**(4), 175-185.

Rochette, P. and Labossière, P. (2000), "Axial testing of rectangular column models confined with composites", *J. Compos. Constr., ASCE*, **4**(3), 129-136.

Wang, L.M. and Wu, Y.F. (2008), "Effect of corner radius on the performance of CFRP-confined square concrete columns", *Eng. Struct.*, **30**, 493-505.

Al-Salloum, Y.A. (2007), "Influence of edge sharpness on the strength of square concrete columns confined with FRP composite laminates", *Compos. Part B: Eng.*, **38**, 640-650.

Lam, L. and Teng J.G. (2003), "Design-oriented stress-strain model for FRP-confined concrete in rectangular columns", *J. Reinf. Plast. Compos.*, **22**(13), 1149-1186.

Wu, Y.F. and Wei, Y.Y. (2010), "Effect of cross-sectional aspect ratio on the strength of CFRP-confined rectangular concrete columns", *Eng. Struct.*, **32**, 32-45

Lam, L. and Teng, J.G. (2004), "Ultimate condition of fiber reinforced polymer-confined concrete", *J. Compos Construct., ASCE*; **8**(6), 539-548.

Mirmiran, A. and Shahawy, M. (1997), "Dilation characteristics of confined concrete", *Int. J. Mech. Cohesive-Frictional Mater.*, **2**(3), 237-49.

Mirmiran, A. and Shahawy, M. (1997), "Behavior of concrete columns confined by fiber composites", *J. Struct. Eng., ASCE*, **123**(5), 583-590.

Wu, G., Wu, Z.S. and Lu, Z.T. (2007), "Design-oriented stress-strain model for concrete prisms confined with FRP composites", *Constr. Build. Mater.*, **21**,1107-1121.

Zhao, T. and Xie, J. (2000), "Experimental study on complete stress–strain relation curve of CFRP confined concrete", *J. Build. Struct.*, **30**(7),40-43

Saadatmanesh, H., Ehasni, M.R. and Li, M.W. (1994), Strength and ductility of concrete columns externally reinforced with fiber composite straps, *ACI Struct. J.*, **91**(4), 434-447.

ACI Committee 440 Report (2002), *Guide for the Design and Construction of Externally Bonded FRP Systems for Strengthening Concrete Structure*s, ACI Committee 440, Technical Committee Document 440.2R-02

Fraldi, M., Nunziante, L., Carannante, F., Prota, A., Manfredi, G. and Cosenza, E. (2008), "On the prediction of the collapse load of circular concrete columns confined by FRP", *Eng. Struct.*, **30**, 3247-3264.

Jiang, T. and Teng, J.G. (2007), "Analysis-oriented stress-strain models for FRP-confined concrete", *Eng. Struct.*, **29**, 2968-86.

Rousakis, T.C., Karabinis, A.I. and Kiousis, P.D. (2007), "FRP-confined concrete members: Axial compression experiments and plasticity modeling", *Eng. Struct.*, **29**, 1343-1353.

Sheikh, S.A. and Li, Y. (2007), "Design of FRP confinement for square concrete columns", *Eng. Struct.*, **29**, 1074-1083.

Harajli, M.H. (2006), "Axial stress-strain relationship for FRP-confined circular and rectangular concrete columns", *Cement Concrete Compos.*, **28**, 938-948.

Binici, B. (2005), "An analytical model for stress-strain behavior of confined concrete", *Eng. Struct.*, **27**(7),

1040-1051.
Lam, L. and Teng, J.G. (2004), "Behavior and modeling of fiber reinforced polymer-confined concrete", *J Struct Eng, ASCE*; **130**(11), 1713-1723.
Xiao, Y. and Wu, H. (2000), "Compressive behavior of concrete confined by carbon fiber composite jackets", *J. Mater. Civil Eng., ASCE*, **12**(2), 139-146.
Spoelstra, M.R. and Monti, G. (1999), "FRP-confined concrete model", *J .Compos. Constr., ASCE*, **3**(3), 143-150.
Samaan, M., Mirmiran, A. and Shahawy, M. (1998), "Model of concrete confined by fiber composite", *J Struct. Eng., ASCE*, **124**(9), 1025-1031.
Pessiki, S., Harries, K.A., Kestner, J.T., Sause, R. and Ricles, J.M. (2001), "Axial behaviour of reinforced concrete columns confined with FRP Jackets", *ASCE J Compos. Construct.*, **5**(4), 237-245.
Abbasnia, R., Hosseinpour, F., Rostamian, M. and Ziaadiny, H. (2012), "Effect of corner radius on stress-strain behavior of FRP confined prisms under axial cyclic compression", *Eng. Struct.*, **40**, 529-535.
Abbasnia, R., Ahmadi, R. and Ziaadiny, H. (2012), "Effect of confinement level, aspect ratio and concrete strength on the cyclic stress–strain behavior of FRP-confined concrete prisms", *Compos. Part B: Eng.*, **43**, 825-831.
Abbasnia, R. and Ziaadiny, H. (2010), "Behavior of concrete prisms confined with FRP composites under axial cyclic compression", *Eng. Struct.*, **32**, 648-655
Shao, Y., Zhu, Z. and Mirmiran, A. (2006), "Cyclic modeling of FRP-confined concrete with improved ductility", *Cement Concrete Compos.*, **28**, 959-968.
Lam, L. and Teng, J.G. (2009), "Stress-strain model for FRP-confined concrete under cyclic axial compression", *Eng. Struct.*, **31**, 308-321.
Lam, L., Teng, J.G., Cheung, J.G. and Xiao, Y. (2006), "FRP-confined concrete under axial cyclic compression", *Cement Concrete Compos.*, **28**(10), 949-958.

CC